Bright source X-ray spectroscopy with XMM-Newton: A modified EPIC-pn Timing mode

Eckhard Kendziorra[*a], Jörn Wilms[b], Frank Haberl[c], Marcus Kirsch[d], Michael Martin[a], Michael A. Nowak[e]

[a]Institut für Astronomie und Astrophysik, Eberhard-Karls-Universität, Sand 1, 72076 Tübingen, Germany
[b]Department of Physics, University of Warwick, Coventry, CV4 7AL United Kingdom
[c]Max-Planck-Institut für extraterrestrische Physik, Giessenbachstr., 85748 Garching, Germany
[d]XMM-Newton Science Operations Centre – VILSPA, Apartado - P.O. Box 50727, 28080 Madrid
[e]MIT-CXC, NE80-6077, 77 Massachusetts Ave., Cambridge, MA, USA

ABSTRACT

The large collecting area of XMM-Newton combined with the good energy resolution of the EPIC-pn CCDs allows the study, with unprecedented detail, of accretion processes onto neutron stars and black holes. The EPIC-pn CCD camera in Timing mode, in which data are read out continuously, is among the fastest X-ray CCD camera available; however, telemetry constraints do not allow full use of these capabilities for many sources because currently randomly distributed data gaps are introduced by the on-board data handling electronics. As an alternative, we have proposed to implement a modification of the Timing mode in which data from soft X-ray events are not transmitted to Earth. Here we discuss the properties of this modified Timing mode, which will first be used in simultaneous XMM-Newton, RXTE, and INTEGRAL observations of the Galactic black hole binary Cygnus X-1 in autumn 2004. We discuss the predicted performance of this new mode based upon laboratory measurements, Monte Carlo simulations, and data from existing Timing mode observations.

Keywords: XMM-Newton, EPIC, pn-CCD, Timing, Cyg X-1

1. INTRODUCTION

XMM-Newton provides the unique opportunity to observe sources simultaneously with high energy resolution below 2 keV with the Reflection Grating Spectrometer (RGS)[1], and with the full grasp of the European Photon Imaging Camera (EPIC)[2], with moderate CCD-type resolution up to 15 keV. Although the EPIC-pn camera provides special modes for the observation of bright Galactic sources (see Chapter 3.1) one presently cannot make full use of the XMM-Newton EPIC collecting area due to telemetry constraints. A small modification of the present camera setting, however, will make this possible. The full sensitivity of EPIC-pn will then allow time resolved spectroscopy around the Iron Kα line at 6.4 keV.

In this paper we present this modified Timing mode for the energy band 2 to 15 keV and discuss its properties for an AO3 observation of the Galactic black hole binary Cygnus X-1. The outline of the paper is as follows: In Section 2 we briefly discuss the science case for an observation of Cyg X-1 with XMM-Newton. In Section 3 we first describe the currently available operating modes of the pn-CCD camera for the observation of bright sources and discuss their limitations, then we introduce the modified Timing mode. The predicted performance for this new mode is discussed in Section 4.

[*] kendziorra@astro.uni-tuebingen.de; phone +49 7071 2976127; fax +49 7071 293458

2. SCIENCE CASE

Due to the multitude of observable phenomena, High Mass X-ray Binaries (HMXBs) provide an especially interesting laboratory for broad-band high resolution X-ray spectroscopy and timing studies of both the stellar wind from the O/B donor star in these systems, as well as of the physical processes close to the compact object.
One of the best known and brightest HMXBs is the Galactic black hole binary HDE226868/Cygnus X-1. It is only now, more than four years after launch, that Cyg X-1 has left the avoidance zone, allowing for the first time high signal-to-noise studies of this prototype black hole candidate with XMM-Newton.

Optical and radio studies of HDE226868/Cyg X-1 indicate that the black hole accretes a fraction of the strong stellar wind of HDE226868 via a "focused stellar wind" [3-6]. The system thus presents a rare intermediate case between systems exhibiting pure spherical wind accretion (such as, e.g., Vela X-1) and Roche Lobe overflow (such as seen, e.g., in low-mass X-ray binaries). Close to the black hole, an accretion disk forms, which is most probably surrounded by a hot electron plasma (the "accretion disk corona"). Soft X-rays from the inner disk (kT_{in} ~ 250 eV) are Compton up-scattered by hot electrons (kT_e ~ 100 keV) in the corona, resulting in a hard power-law spectrum with photon index Γ~ 1.7 and an exponential cutoff at ~ 150 keV. Part of these hard photons are intercepted by the comparably "cold" material of the accretion disk, giving rise to a Compton reflection hump at ≥ 8 keV and to fluorescent Fe Kα emission at 6.4 keV[7].

Some of the major advances in our knowledge of the radiation processes of Galactic black holes have come from both spectral and variability observations performed with the >1000 cm^2 proportional counter array (PCA) on *RXTE*. Due to its low energy resolution, many studies, e.g., the detailed structure of even broad fluorescent Fe Kα features or variability in narrow bands (i.e., isolating the variability of the Fe line region from that of the continuum[8]), are difficult as only several keV wide energy bands can be studied. CCD-resolution spectroscopy with the EPIC-pn camera does not suffer from these problems. EPIC-pn also detects the Fe line and edge region with far greater effective area than *Chandra*.

An XMM-Newton observation of Cyg X-1 will therefore yield unprecedented insight into the behavior and physics of Galactic black holes. In detail, one can study the following issues:

- Study the spectra below 2 keV with the Reflection Grating Spectrometer (RGS)
- Determine the 2-15 keV continuum shape with EPIC-pn, while modeling the reflection features using the RGS derived abundances
- Search for structure of the Fe line, such as the presence of relativistic broadening similar to that observed by XMM-Newton in MCG-6-30-15[9, 10]
- Measure energy resolved power spectra (PSDs) to study the energy dependence of the Lorentzian components that have recently been found to be a good description of the PSDs of neutron stars and black holes, e.g. Pottschmidt et al. (2002 and references therein) [11], with higher energy resolution than that of the *RXTE*.

3. EPIC PN-CCD OPERATING MODES FOR BRIGHT SOURCES

3.1 Currently available modes for the observation of bright sources

The observation of bright sources with imaging spectrometers, like the EPIC CCD cameras, is limited by telemetry bandwidth and pile-up. With X-ray CCDs the energy of a photon is measured by the amount of charge generated in the detector. The charge cloud can either be collected entirely within one pixel (single event) or split among more than one pixel (split event). For a given surface brightness on the detector, one has to read out the CCD fast enough to keep the probability below a certain level for charge clouds from two or more photons falling into the same pixel (called energy

pile-up) or being tangent to each other (called pattern pile-up). This so-called "pile-up limit" further depends on the number of pixels sampling the point spread function (PSF).
Consequently, for the observation of brighter sources and/or if a time resolution of better than 6 ms is required, the pn-CCD can be operated in special fast readout modes, where the shorter readout times are achieved on the expense of reduced spatial information. Two fast readout modes are currently available for EPIC-pn, the so-called Timing and Burst modes. In both cases only the focus CCD (CCD 4) is read. For a more detailed description of these modes see Kendziorra et al. 1997[12] and Kendziorra et al. 1998[13].

Table 1. Pile-up and telemetry limits for Timing and Burst mode and life time of these modes.

Mode	Pile-up limit [cts/s]	Telemetry limit [cts/s]		Life time [%]
Allocated telemetry		16 kbit/s	40 kbit/s	
Timing	1,500	250	1,050	99.5
Burst	60,000	~13,000	~40,000	3

In Timing mode the CCD is read out continuously, integrating the charge of 10 pixels in so-called macro pixels of 0.15 mm x 1.5 mm size. A row of 64 macro pixels is read out within 29.52 μs. This results in a high time resolution (and short integration time under the PSF) of ~30 μs and thus the pile-up limit is much higher than for imaging modes. The pile-up limit for Timing mode is 1500 cts/s. However, due to telemetry limitations this mode can only be used up to 1 k events/s at the most without losing events during so-called counting mode intervals (see Figure 1).

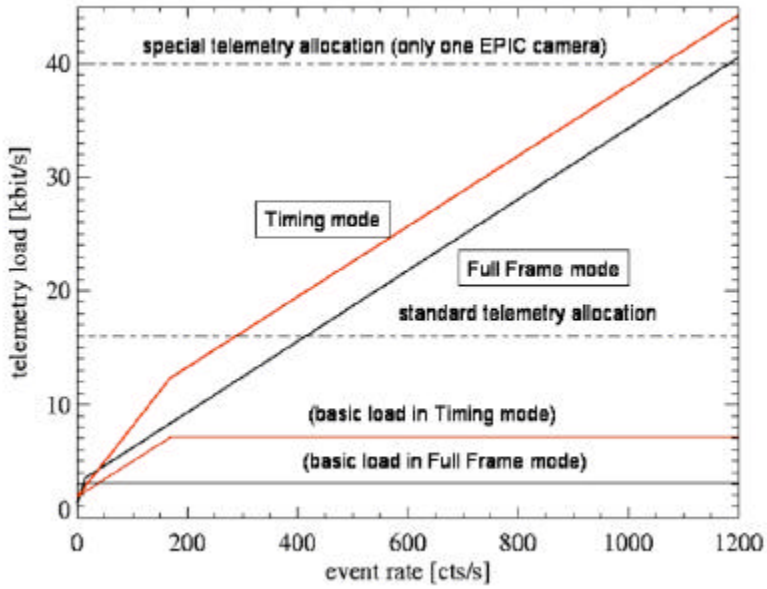

Figure 1. Telemetry bit rate vs. event rate for Timing and Full Frame mode, the basic load is caused by forced transmission of time and event counter information every 20 CCD readout frames.

For brighter sources, the Burst mode would be appropriate, where the CCD is used like an analogue transient recorder for very short observation intervals separated by much longer readout intervals. The high transfer speed of 0.720 μs/row during exposure intervals minimizes the integration time under the PSF, keeping the probability for pile-up low, even for sources as bright as six times the Crab. However, this mode is only suitable for the observation of very bright point sources, because the effective exposure time (called life time in Table 1) is only 3 %. In addition, Burst mode is not appropriate for PSD studies, due to its extreme window function[14].
For a ~300 mCrab source, such as Cyg X-1 in the hard state, the standard Timing as well as Burst mode would significantly reduce the signal to noise ratio due to counting mode intervals or extremely low life time. Thus, all the

generic XMM-Newton science, such as Fe line and continuum variability studies, where the large collecting area of XMM-Newton is needed, would severely be hampered.

3.2 Modified Timing Mode

As there are no EPIC MOS data modes available which can accommodate a source as bright as Cyg X-1, the MOS can be switched off and the full ~40 kbps telemetry can be allocated for the EPIC-pn. This results in a maximum count rate of 1050 cps before pn data are lost due to counting mode intervals. (The EPIC cameras autonomously switch into counting mode as soon as their event buffer is filled by more than 75%. Events recorded during these intervals are only counted but not transmitted to ground. Normal operation is resumed when the buffer level reaches 25%.)
Simply raising the lower event threshold from 200 eV in standard Timing mode to 2.2 keV will reduce the count rate from Cyg X-1 to ~900 cps, while leaving a safety margin for the possibility that the observation will be performed during the softer and brighter "failed state transitions". Laboratory measurements show that for a 300 mCrab source the energy pile-up will be less than 1%[13]. Pattern pile-up and the changed lower energy threshold, however, change the distribution of single and double events, necessitating the generation of new response matrices.
Based on laboratory measurements, in orbit data and simulations we will discuss in Section 4 the predicted performance of the modified Timing mode in terms of energy resolution, pattern distribution, and pile-up.

4. PREDICTED PERFORMANCE OF THE MODIFIED TIMING MODE

4.1 Energy resolution and redistribution

For the calibration of Timing and Burst mode measurements at the MPE long beam test facility (Panter) have been performed in December 2000, using the EPIC-pn spare camera (Kirsch 2003[15]). Deep flat field exposures of fluorescence K and L lines were taken at 11 energies in Full Frame mode and in Timing mode (see Table 2). All measurements were done with a lower threshold of 16 ADU, equivalent to 80 eV (1 ADU = 5 eV).

Table 2. Lines and their energies to be used for the calibration of the modified Timing mode

Element-Transition	Energy in keV	Element-Transition	Energy in keV
O-Kα	0.525	Mo-Lα	2.293
Fe-Lα	0.705	Ag-Lα	2.984
Ni-Lα	0.930	Ti-Kα	4.511
Mg-Kα	1.254	Fe-Kα	6.404
Al-Kα	1.487	Cu-Kα	8.048
Si-Kα	1.740		

These archival data sets will be used to build the energy response matrix for the modified Timing mode. In this paper we discuss the influence of an increased lower threshold on the energy resolution and redistribution.
As an example we show in Figure 2 and Figure 3 the Si-Kα spectra (1.740 keV) of single events for five different lower thresholds, ranging from 80 eV (16 ADU) to 1.2 keV (240 ADU), for Full Frame and Timing mode, respectively. The effect of an increased lower threshold (LT) can best be seen in Full Frame mode because here the percentage of split events is much higher as compared to Timing mode, see Chapter 4.2 for more details.
While the spectral shape is quite symmetrical at LT = 80 eV, already at LT = 200 eV (the setting of the standard Timing mode) the red wing of the line develops a shallow shoulder. This originates from split events where the low energy part falls below the threshold; these events are thus wrongly recorded as singles (called "pseudo singles" by some authors). One nicely can see this effect in the cases of LT = 80 ADU and LT = 160 ADU, where the spectrum of single events follows the spectrum of all events (Figure 4) down to an energy $E_c = E_l - E_{LT}$, where E_l is the line energy and E_{LT} is the energy of the lower threshold. For a lower threshold above $E_l/2$, 1.2 keV in our example, part of the flat shoulder stemming from split events is already cut off by the lower level discriminator.

While the energy redistribution strongly depends on the lower threshold chosen, the energy resolution is only marginally affected by a higher threshold, provided the threshold is well below the line energy. For Cyg X-1 we are mainly interested in a high efficiency and good energy resolution at the Fe-Kα line. To prove that the modified Timing mode

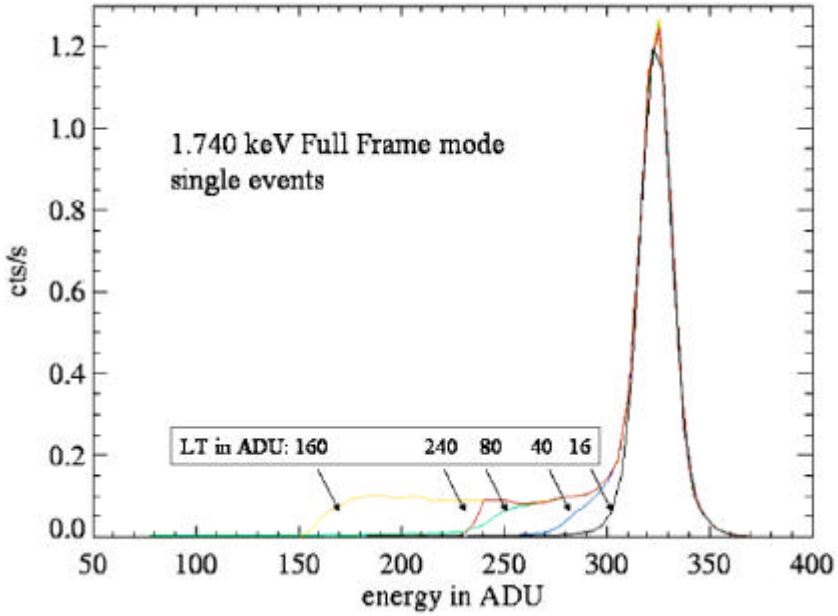

Figure 2. 1.740 keV single spectrum of Si-Ka in Full Frame mode for different lower thresholds: 16 ADU (80 eV), 40 ADU (200 eV), 80 ADU (400 eV), 160 ADU (800 eV), and 240 ADU (1.2 keV)

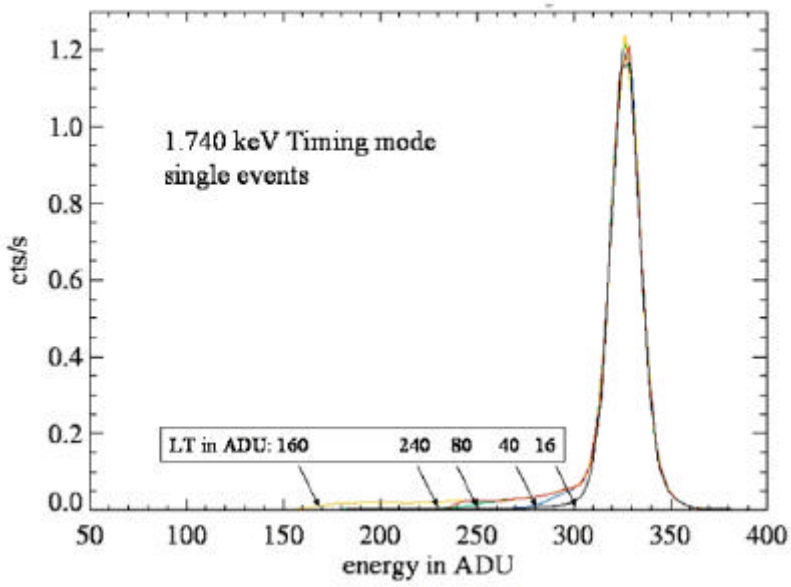

Figure 3. 1.740 keV single spectrum of Si-Ka in Timing mode for different lower thresholds: 16 ADU (80 eV), 40 ADU (200 eV), 80 ADU (400 eV), 160 ADU (800 eV), and 240 ADU (1.2 keV)

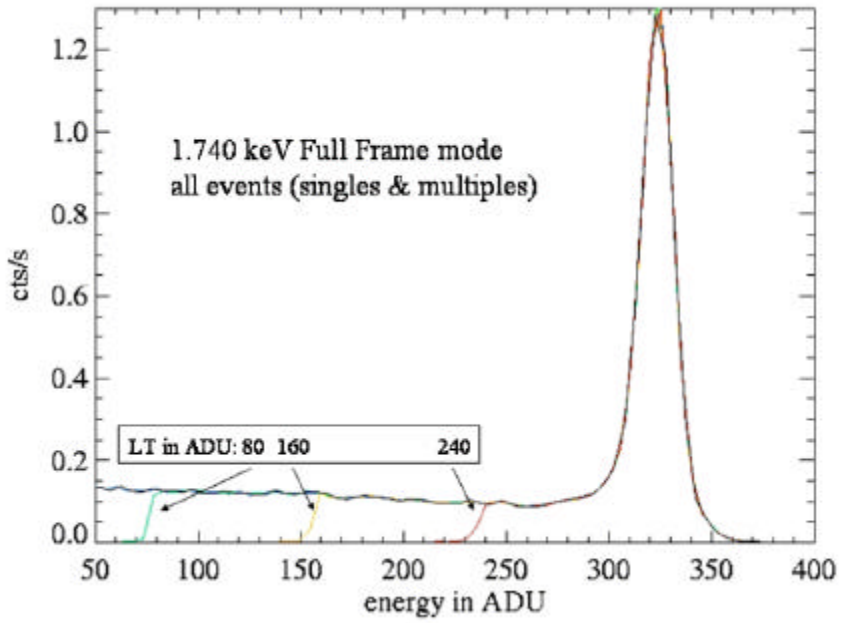

Figure 4. 1.740 keV spectrum of all events, lower thresholds: 80 ADU (400 eV), 160 ADU (800 eV), 240 ADU (1200 eV)

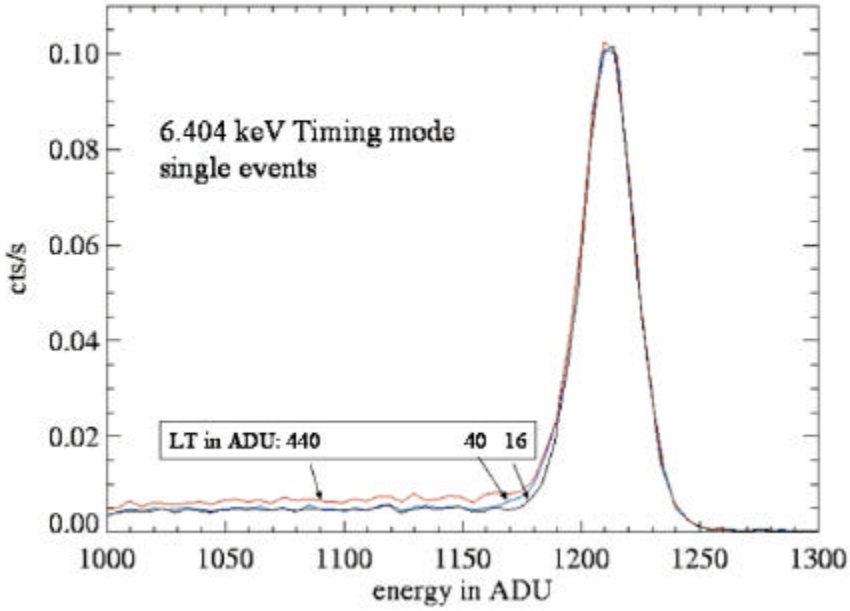

Figure 5. 6.4 keV single event spectrum of Fe-Ka in Timing mode for LT: 16 ADU (80 eV), 40 ADU (200 eV), and 440 ADU (2.2 keV)

fulfills these requirements we show in Figure 5 the laboratory Fe-Kα spectrum with three different LT applied; 80 eV, 200 eV, the setting of the standard Timing mode, and 2.2 keV the setting anticipated for the modified Timing mode observation of Cyg X-1. This result nicely demonstrates the ability of the modified Timing mode for the observation of Fe lines.

4.2 Pattern distribution

For the correct deconvolution of spectra the energy dependent fraction of single events, double events and events spread over more than two pixels has to be known, since this fraction enters into the detector response matrix due to the different energy redistribution of double events. As already discussed previously, this distribution depends on the lower threshold and on the pixel size. In Figure 6 we show the fraction of single events and double events for the measurements of the 11 line energies from Table 2 for Full Frame and Timing mode. As the dimension of the charge cloud only depends on the photon energy and not on the operating mode, from simple geometrical considerations one would expect a factor of ~2 less multiple events in Timing mode as compared to Full Frame mode. The measurements, however, reveal an even smaller fraction of multiple events in Timing mode. The reason for this smaller fraction of multiple events is the asymmetrical distribution of split events in the pn-CCD. The number of doubles along the shift direction is about a factor of two larger than perpendicular to it. In Timing mode, however, 90% of doubles along the shift direction are recombined in one single macro pixel. This split asymmetry has recently been explained in detail by Englhauser et al.[16].

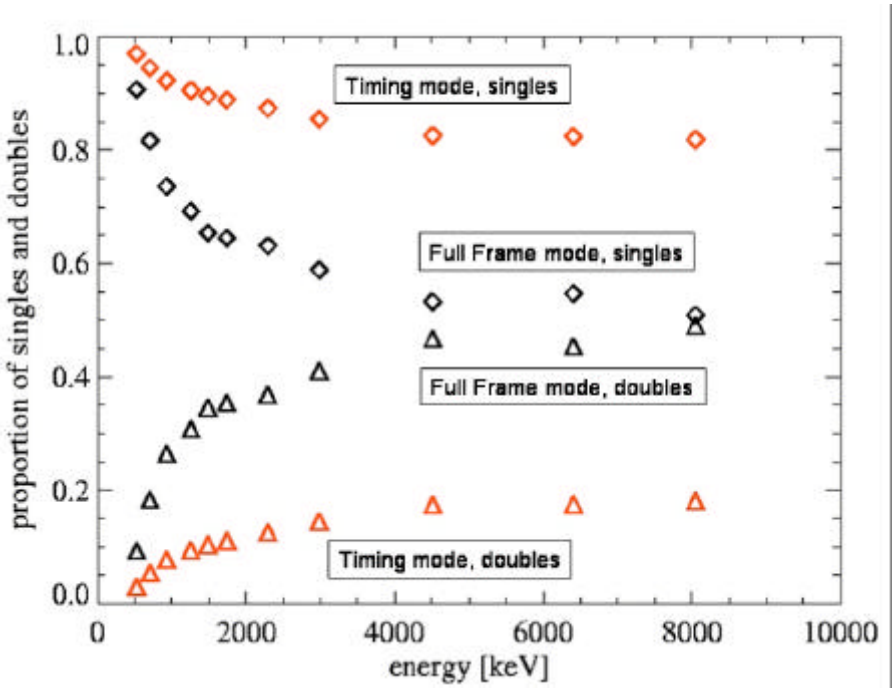

Figure 6. Distribution of single and double events in Full Frame and Timing Mode

To investigate how the split distribution changes as function of lower threshold for a ~300 mCrab source, we analyzed archival Timing mode data from a Crab observation in XMM-Newton's revolution 411. Figure 7 shows the measured intensity distribution in RAWX direction perpendicular to the columns. For our analysis we selected data from RAWX columns 18-27 and 40-51, where the surface brightness on the CCD is similar to the value we expect for our Cyg X-1 observation. We then generated two data sets, one with the standard LT at 200 eV, and one with LT set to 2.2 keV. The energy dependent pattern distributions for both LT values extracted with a software similar to the XMM Standard

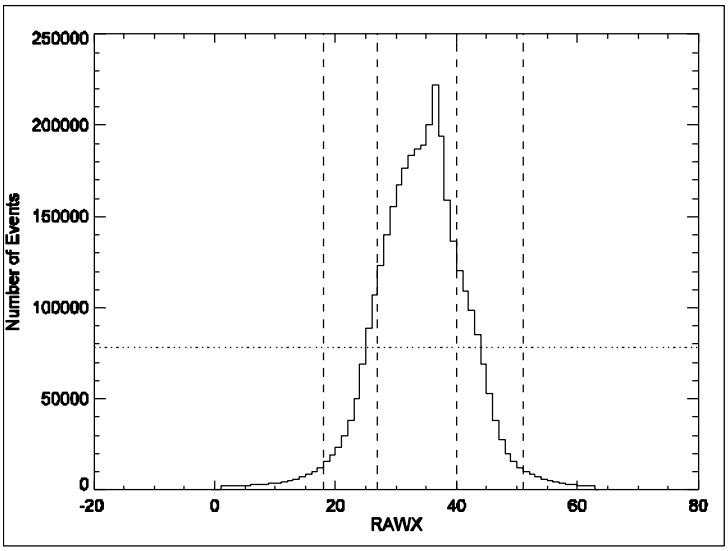

Figure 7. Measured intensity distribution along the RAWX direction (columns) for the Timing mode observation of the Crab in revolution 411, columns inside the dashed areas left and right from the peak have been used to simulate a ~250 mCrab source.

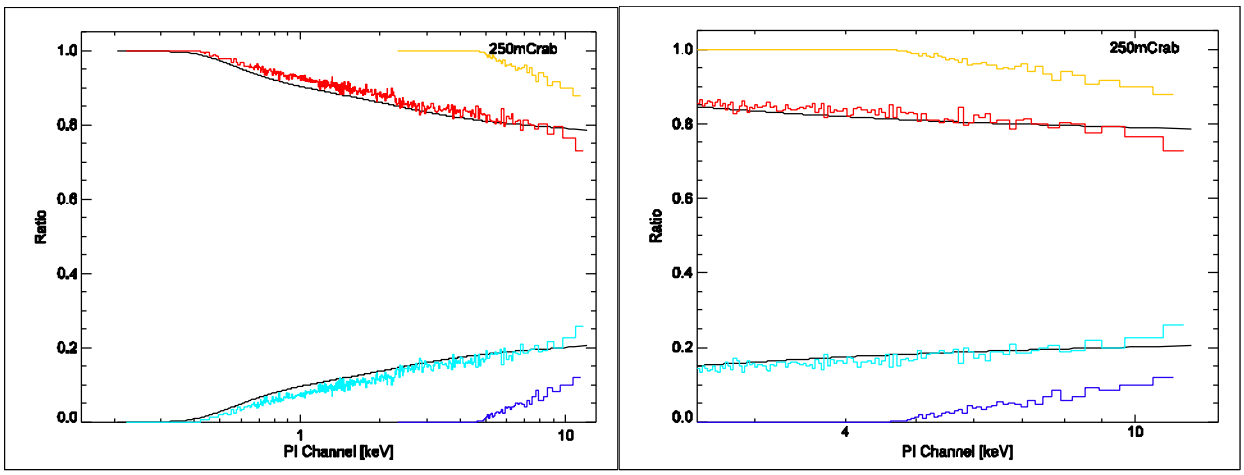

Figure 8. Measured distribution of single (top curves) and double events (bottom curves) as function of energy for a ~250 mCrab source with lower threshold at 200 eV (40 ADU), here the expected distribution is plotted as well, and 2.2 keV (440 ADU), starting at 2.2 keV for singles and 4.4 keV for doubles; left: full energy range, right: above 2.2 keV.

Analysis System (SAS) tool EPATPLOT are shown in Figure 8, together with the expected single and double distribution for the LT=200eV case. Measurements such as this one will allow us to determine the expected single and

double distribution for the LT=2.2keV value of the observation of Cyg X-1, which as expected is very different from the standard distribution. As mentioned above, we will be using this distribution to adapt the response matrix for the modified Timing mode accordingly. We note that there is a slight discrepancy between the observed and predicted single to double distribution for the LT=200eV case, indicating a higher fraction of single events than expected. This is a well known issue of the current Timing mode calibration. We stress that more importantly the measured single and double distribution for the LT=200eV case does not show a clear indication for pile-up, and thus our observation of Cyg X-1 will not be piled up. This will allow us to determine the continuum shape of Cyg X-1 above 2.2 keV sufficiently well.

4.3 Effect of pile-up on continuum and Iron Kα line

From Figure 8 we deduce that for a ~300 mCrab source the shape of the continuum would only marginally be affected by pile-up. In order to verify that this is also true for the position and width of the Iron Kα line in Cyg X-1 we have run Monte Carlo simulations.

The readout of the pn CCD in Timing mode was simulated using a slightly modified version of our simulation program for the assessment of fast read out detectors for the XEUS fast timing channel, see Wilms et al.[17] in this volume.

The spectrum of Cyg X-1 was modeled by a power law continuum (?=1.7) plus a narrow Iron Kα line at 6.4 keV. From the spectrum we generated a light curve by randomly sorting the events in time bins of 29.5 μs each. Events within a time bin were then distributed on the detector simulating the intensity distribution of a PSF with 15 arcsec half energy

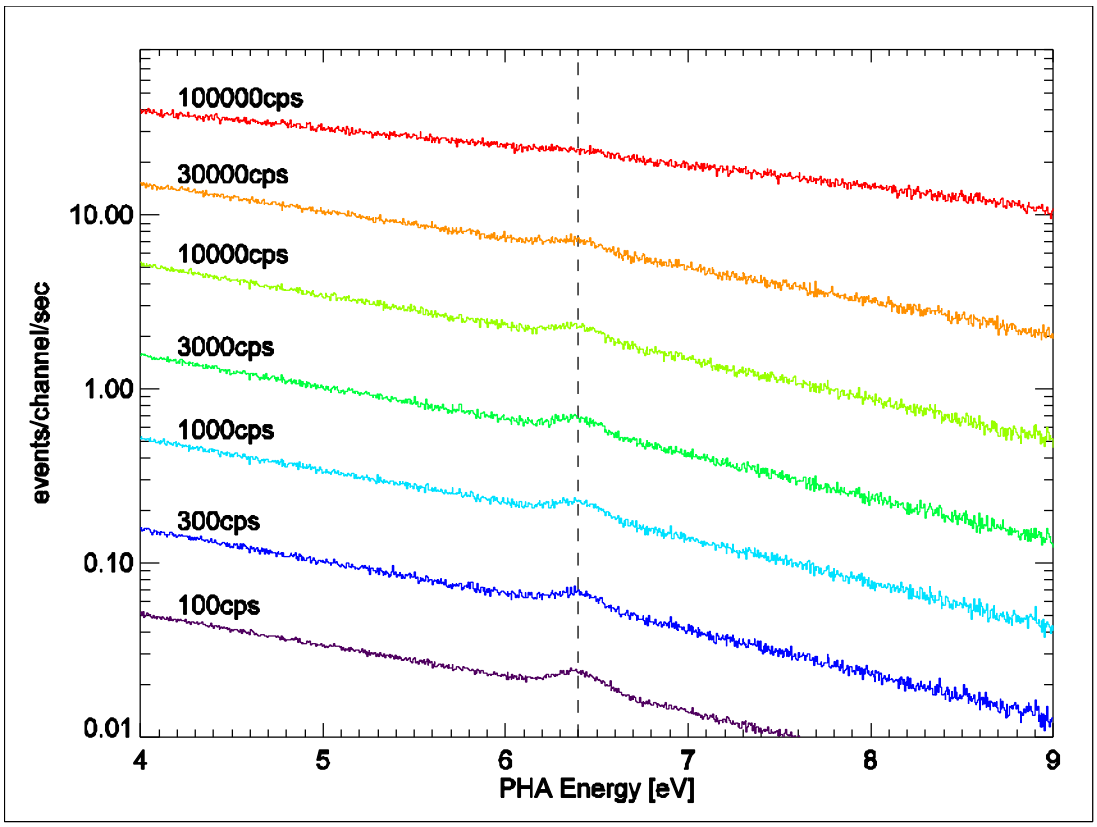

Figure 9. Simulated Iron Ka line for seven source intensities from 300 cps to 100,000 cps

width. Using the measured pattern distribution we then simulated the charge distribution in the detector plane. Thus the effect of pattern and energy pile-up was accounted for. In Figure 9 we show the resulting spectra around 6.4 keV for seven source intensities, ranging from 100 cts/s (well below the pile-up limit of Timing mode) up to 100,000 cts/s, where the measured spectrum is heavily distorted by pile-up. As predicted the shape of the continuum and width of the Iron line stay the same at least up to a flux of 3000 cts/s, confirming that the study of the position and shape of the Cyg X-1 iron line is not hampered by pile-up.

5. CONCLUSIONS

The proposed modified Timing mode will allow to study Iron lines and the continuum above ~2.2 keV of bright sources with unprecedented statistical accuracy and time resolution.
After our observation of Cyg X-1 in autumn this year, we will fully calibrate this mode and make the response matrix available to the public.

ACKNOWLEDGEMENTS

This project is supported by Deutsches Zentrum für Luft- und Raumfahrt (DLR).

REFERENCES

1. den Herder J.W. et al., 2001, A&A, 356, L7
2. Strüder L. et al., 2001, A&A, 356, L18
3. Tarasov A.E., Brocksopp C., Lyuty V.M., 2003, A&A 402, 237
4. Gies D.R., Bolton C.T., Thomson J.R., et al., 2003, ApJ 583, 424
5. Brocksopp C., Fender R.P., Larionov V., et al., 1999, MNRAS 309, 1063
6. Gies D.R., Bolton C.T., 1986, ApJ 304, 389
7. Magdziarz P., Zdziarski A.A., 1995, MNRAS 273, 837
8. Maccarone T.J., Coppi P.S., 2002, MNRAS 335, 465
9. Wilms J., Reynolds C.S., Begelman M.C., et al., 2001, MNRAS 328, L27
10. Fabian A.C., Vaughan S., Nandra K., et al., 2002, MNRAS 335, L1
11. Pottschmidt K., Wilms J., Nowak M.A., et al., 2003, A&A 407, 1039
12. Kendziorra E. et al., 1997, Proc. SPIE 3114, 155
13. Kendziorra E. et al., 1998, Proc. SPIE 3445, 50
14. Kuster M. et al., 1999, Proc. SPIE 3765, 673
15. Kirsch M. PhD thesis University of Tübingen, 2003
16. Englhauser J. et al., 2004, Proc. SPIE 5501, to be published
17. Wilms J. et al., 2004, Proc. SPIE, this volume